Investigation of the elastic properties of $LiKSO_4$ as a function of temperature and pressure

2003 J. Phys.: Condens. Matter 15 4979

(http://iopscience.iop.org/0953-8984/15/29/309)

INSTITUTE OF PHYSICS PUBLISHING JOURNAL OF PHYSICS: CONDENSED MATTER

J. Phys.: Condens. Matter **15** (2003) 4979–4993 PII: S0953-8984(03)58387-4

Investigation of the elastic properties of $LiKSO_4$ as a function of temperature and pressure

G Quirion[1], M Abu-Kharma[1], I A Sergienko[1], M Bromberek[1], M Clouter[1] and B Mroz[2]

[1] Department of Physics and Physical Oceanography, Memorial University, St John's, NL, A1B 3X7, Canada
[2] Institute of Physics, Adam Mickiewicz University, Poznan, Poland

E-mail: gquirion@physics.mun.ca

Received 16 January 2003, in final form 12 June 2003
Published 11 July 2003
Online at stacks.iop.org/JPhysCM/15/4979

Abstract

In spite of the large number of reports on the physical properties of $LiKSO_4$, its low-temperature phase diagram is still not well defined. One possible reason for this lack of reliable data below 100 K might be that $LiKSO_4$ crystals often break into many pieces when cooled below 80 K under atmospheric pressure. We have found that it is possible to thermally cycle $LiKSO_4$ crystals, particularly at temperatures below 80 K, as long as a minimum pressure of about 0.5 kbar is maintained. Thus, we successfully measured the temperature dependence of the sound velocity between 4 and 300 K for pressures up to 7 kbar. Over that temperature range, we clearly identify five different phase transitions (37, 48, 65, 185, 195 K) which correspond to those observed by other groups using different techniques. However, our results also show that both phase transitions below 50 K are strongly suppressed at pressures greater than 3 kbar. A Landau model of the free energy, based on the group theory, is also presented in order to explain the elastic and dielectric properties of $LiKSO_4$ above 100 K. To support our analysis, we show how this model accounts for the temperature dependence of the strains, polarizations, dielectric susceptibility and elastic constants.

1. Introduction

The physical properties of $LiKSO_4$ have been extensively studied and it is now well established that this ferroelastic compound exhibits a rich variety of structural phase transitions. Above 943 K it is well established that the crystal structure of $LiKSO_4$ is hexagonal and belongs to the space group designation $P6_3/mmc$ [1, 2]. The structure of the phase between 708 and 943 K is still uncertain but it seems to be incommensurate. At room temperature $LiKSO_4$ has been extensively studied, and its structure is convincingly described by the hexagonal

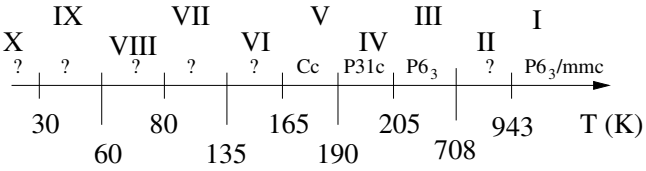

Figure 1. Schematic diagram of the phase transition temperatures in $LiKSO_4$ as proposed by Perpétuo *et al* [10].

$P6_3(C_6^6)$ space group [3, 4]. With further decrease in temperature, $LiKSO_4$ undergoes a first-order phase transition around 205 K. After some controversies, it is now believed that the proper structure of the phase observed between 190 and 205 K is trigonal ($P31c$) rather than hexagonal ($P6_3mc$) [5–7]. The phase transition at 205 K is followed by another first-order phase transition at 190 K which transforms the crystal into the monoclinic Cc space group. At lower temperatures several other phase transitions, possibly related to the dynamics and the reorientation of the SO_4 tetrahedra, have been observed. However, in spite of extensive experimental work (see [8] and [9] for a literature review), a definitive picture of the actual number of phases and transition temperatures, as well as their structural nature, is still lacking. All these results have been used by Perpétuo *et al* [10] to derive a hypothetical phase diagram for $LiKSO_4$. For convenience, we reproduce that diagram in figure 1 along with the transition temperatures which are obtained after averaging over published values for cooling runs only. As we can see, this figure indicates up to 10 possible phases. However, only the structure of the high-temperature phases have been clearly identified so far.

Brillouin scattering [11–16] and ultrasonic velocity measurements [17–21] have played a significant role in the determination of the unusual elastic properties of $LiKSO_4$. However, all these investigations, except for one [15], have been limited to temperatures above 100 K so that very little is known about the elastic properties of $LiKSO_4$ at low temperatures. Thus, one of our aims in this investigation was to detect the low-temperature phase transitions for which controversies still remain. This was realized using an acoustic interferometer which allows us to measure variations in the sound velocity as small $\Delta V/V = 10^{-6}$. In comparison with previous sound measurements on $LiKSO_4$, our resolution is at least two or three orders of magnitude greater. Moreover, these measurements have been realized under pressure which allow us to derive the pressure–temperature phase diagram of $LiKSO_4$. The measurements presented here cover the temperature range between 4 and 300 K for pressures up to 7 kbar. Finally, in section 4, we also present a Landau model derived from group theory principles. In particular, we show how this model successfully predicts the elastic as well as the dielectric properties of $LiKSO_4$ in the case of the $P31c$–Cc phase transition.

2. Experiment

The lithium–potassium sulphate single crystals used in this study were grown from an aqueous solution in the Crystal Physics Division, Faculty of Physics at the Adam Mickiewicz University in Poznan (Poland). The solution contained an equimolar proportion of K_2SO_4 and Li_2SO_4 salts. The crystals were grown under isothermal conditions at 315 K by slow evaporation. The grown crystals all had a hexagonal shape which allowed for an immediate identification of the c-axis. Rectangular shaped samples ($\sim 4 \times 4 \times 4$ mm^3) were cut from untwinned parts of the crystal. The parallel faces, with normal axis parallel or perpendicular to the c-axis [001], were then ground and carefully polished to minimize the acoustic losses due to diffraction effects.

All samples used were of good optical quality, and prior to the experiment, their orientation was confirmed using polarized light. Initially we attempted to measure the sound velocity in $LiKSO_4$ using a 30 MHz longitudinal piezoelectric transducer that was bonded to the crystal. However, due to the strong deterioration of the mechanical coupling between the transducer and the sample as we reached 200 K, we rapidly found that this conventional approach to mounting the transducer was not reliable. According to x-ray measurements [22, 23], around 200 K the c-axis and a-axis lattice parameters of $LiKSO_4$ suddenly change by 0.3 and 0.6% respectively. Thus, due to these large thermal contractions, stress builds up within the glue which explains why we systematically lose the acoustic signal around the phase transition. For this investigation, we used a liquid instead of a glue as the acoustic medium between the transducer and the sample. After trying different liquids, we chose a 3-methyl-1-butanol solution which has a freezing temperature of 123 K, well below 200 K. As no stress builds up at the sample–transducer interface, very reproducible results were obtained in that way. Another advantage related to this liquid is that it can also be used as a pressure-transmitting medium. Therefore, all our measurements have been conducted with the sample mounted inside a Cu–Be pressure cell filled with 3-methyl-1-butanol. To maintain the transducer over the sample, a small spring-loaded tip was used. During the experiment, the pressure was constantly monitored using the resistivity change of a lead (Pb) wire mounted next to the sample. The sound velocity was measured using a pulsed acoustic interferometer which is designed to detect variations as small as $\Delta V/V = 1$ ppm. Longitudinal waves propagating either parallel or perpendicular to the c-axis were generated at 30 MHz using $LiNbO_3$ piezoelectric transducers.

3. Results

Based on the time of flight measured between consecutive echoes, we determined the room-temperature velocities of transverse and longitudinal waves propagating parallel and normal to the c-axis. The relation between these velocities and the elastic constant C_{11}, C_{33}, C_{44}, C_{66} were obtained by solving the Christoffel equations considering that the crystal symmetry of $LiKSO_4$ is hexagonal at 300 K. Our results, not shown here, agree very well with previous results obtained by the ultrasonic pulse echo overlap method [20, 24] as well as Brillouin light scattering experiments [11, 13]. In order to measure the sound velocity as a function of temperature, the sample was placed in the pressure cell containing a 3-methyl-1-butanol solution which acts as a hydrostatic pressure-medium. However, for measurements at ambient pressure no force was applied on the piston. In figures 2(a) and (b), we compare the temperature dependence of the relative velocity $\Delta V/V$ obtained for longitudinal modes propagating perpendicular and parallel respectively to the c-axis. For convenience, the results have been normalized relative to the velocity measured at room temperature. For longitudinal waves propagating perpendicular to the c-axis (see figure 2(a)), as the temperature is decreased, the velocity shows two step-like variations, respectively at 186.7 ± 0.1 and 195 ± 1 K. However, during the heating process these two anomalies shift to 195.6 ± 0.1 and 260.5 ± 0.5 K respectively. These critical temperatures obtained for the cooling/heating cycle correspond well with the phase transitions already identified [8–10, 22, 23, 25, 26]. Thus, the rapid variations in the sound velocity coincide with the III–IV and IV–V phase transitions shown in figure 1. Moreover, our measurements confirm the results obtained by Borisov *et al* [18], Kabelka and Kuchler [20] and Drozdowski and Holuj [14] which all show a reduction of about 10% in the velocity as the sample is cooled below 180 K. Surprisingly, while measurements perpendicular to the c-axis show both phase transitions around 200 K, results associated with longitudinal modes propagating along the c-axis (see figure 2(b)) show only one discontinuity in the velocity. Using absolute sound velocity measurements, we estimate this variation to

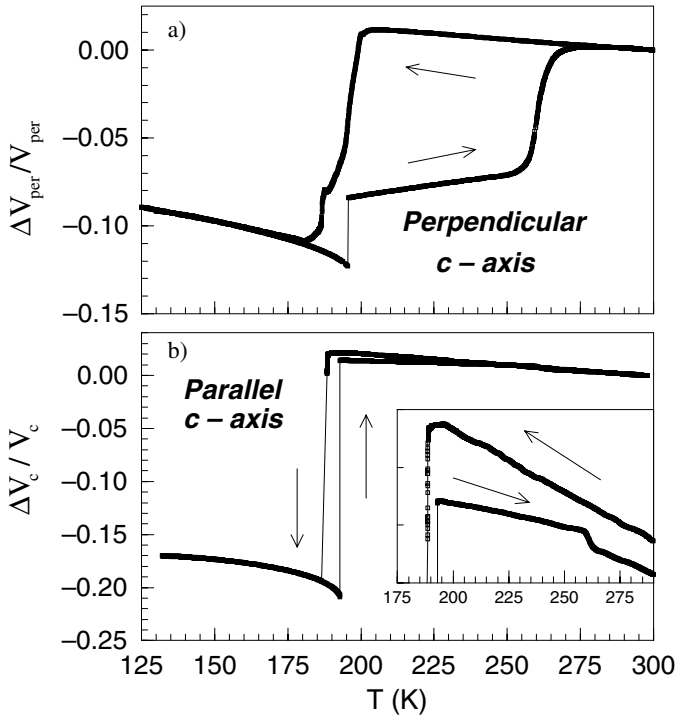

Figure 2. Relative variation of the sound velocity as a function of temperature for $LiKSO_4$: (a) longitudinal waves propagating perpendicular to the *c*-axis, (b) longitudinal waves propagating along the *c*-axis. In the inset, the curves have been shifted relative to each other in order to clearly show the anomaly around 260 K.

be of the order of $22 \pm 5\%$. On cooling, the discontinuity is observed at 188 ± 1 K while for the heating process we observe the discontinuity at 192.8 ± 0.1 K followed by a much smaller change (<0.3%) at 261.2 ± 0.5 K. Consequently, the large velocity variation along the *c*-axis can easily be associated with the IV–V phase transition with no significant variation in the *c*-axis velocity related to the III–IV phase transition at 195 K. Thus our results, as well as results obtained by other groups [14, 20], confirm that the III–IV phase transformation has very little influence on the elastic properties along the *c*-axis. This suggests that the structural reorganization at the III–IV boundary is essentially limited to the xy plane. At lower temperatures (between 125 and 180 K), according to the phase diagram presented in figure 1, one should expect to see two additional anomalies in the elastic properties of $LiKSO_4$. However, our high-resolution sound measurements, along two different directions, do not show any significant variations around 135 and 165 K. Thus, our measurements do not support the existence of structural phase transitions at 135 and 165 K.

We also present in this paper the results of our investigation on the elastic properties of $LiKSO_4$ as a function of pressure. We first present in figure 3 results obtained between 130 and 300 K. These results were obtained using longitudinal waves propagating perpendicular to the *c*-axis. This particular configuration was favoured relative to any others simply because both transitions are easily observed in this case. Considering that large thermal hysteresis is always observed above 150 K, a slow cooling or heating rate of 0.1 K min^{-1} was used throughout the transition temperature range. This was necessary in order to obtain a reliable determination of the critical temperatures as a function of pressure. Due to the thermal contraction of

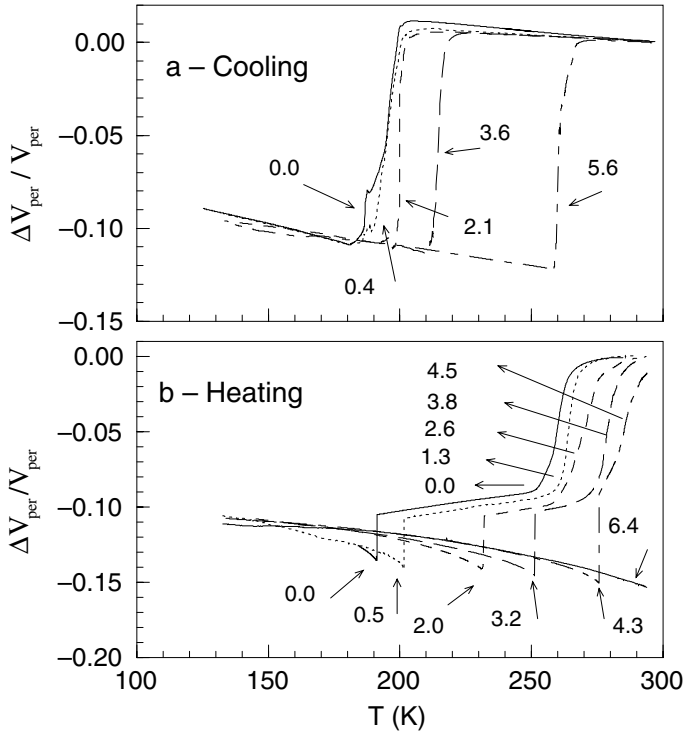

Figure 3. Temperature dependence of the relative change in sound velocity for longitudinal modes propagating perpendicular to the *c*-axis at different pressures (a) on cooling and (b) on heating. Pressures (in kbar) reported here correspond to the pressure measured at the transition temperature.

the different elements of the pressure cell, the pressure was also carefully monitored as a function of temperature. Therefore, the pressures reported in figure 3 correspond to the actual pressure at which the different transitions occur. From these results, the high-temperature part of the pressure–temperature phase diagram of $LiKSO_4$ was derived and is presented in figure 4. Our phase diagram reveals that the intermediate phase IV is suppressed at (200 ± 1 K, 1.8 ± 0.2 kbar) on cooling or (293 ± 2 K, 5.2 ± 0.2 kbar) for the heating process. These temperature–pressure coordinates correspond to those of a triple point where phases III, IV and V coexist. $LiKSO_4$ has been the object of only a few investigations under hydrostatic pressure [25, 27–29]. To our knowledge, the only other pressure–temperature phase diagram for $LiKSO_4$ has been obtained by Fujimoto *et al* [25, 27] using dielectric and dilatometric measurements. From their measurements between 180 and 300 K, they derived a pressure–temperature phase diagram that agrees well with our results. For an easier comparison, we present in table 1 the critical temperatures and pressure coefficients obtained in this work with those of Fujimoto *et al* [25]. The difference in the pressure coefficients reported in table 1 might be attributed to the sample quality, where it seems that even T_c is sample dependent.

The elastic properties of $LiKSO_4$ have been extensively investigated by ultrasonic techniques [17, 19–21] and Brillouin scattering measurements [12–14]. However, none of these investigations were pursued below 80 K. During our preliminary investigation at ambient pressure, we noticed that samples which were cooled down below 60 K show fissures and defects. This might explain why, below 80 K, most results on $LiKSO_4$ are controversial or hardly reproducible. Thus, in order to maintain the samples intact, free of defects or

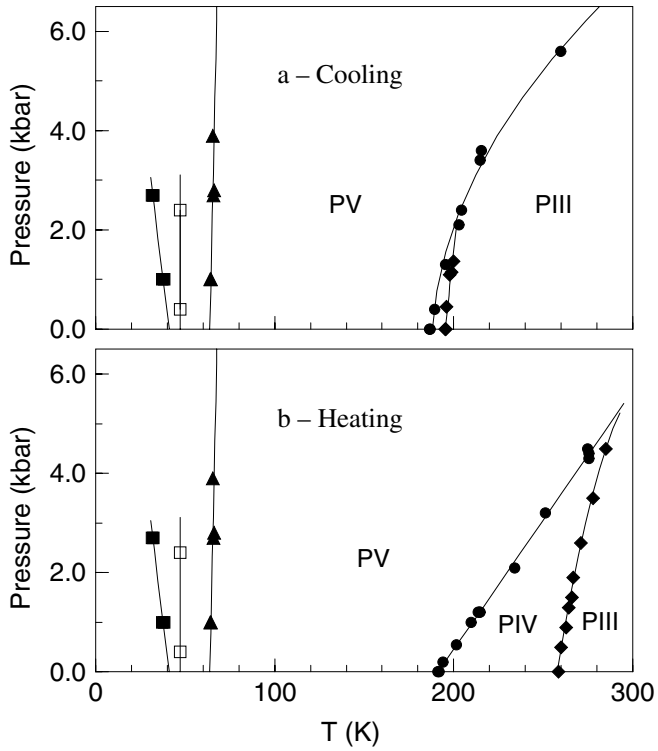

Figure 4. Pressure–temperature phase diagram of $LiKSO_4$ for (a) cooling and (b) heating processes.

Table 1. A comparison of the present work with previous results on the phase diagram of $LiKSO_4$.

Comparison		Present work	Reference [25]
Triple	Cooling	(1.8 kbar, 200 K)	(2.1 kbar, 214 K)
point	Heating	(5.2 kbar, 293 K)	(4.3 kbar, 290 K)
	PIII to PIV	3.0 ± 0.4	2.2 ± 0.4
dT_c/dP	PIII to PV	16 ± 2	11.2 ± 0.3
(K kbar^{-1})	PIV to PV	7.6 ± 0.3	12.0 ± 0.3
	PV to PIV	19.1 ± 0.2	22.2 ± 0.2
	PIV to PIII	5.9 ± 0.3	9.0 ± 0.3

fissures, we systematically cooled them down under pressure. We also found that only results obtained at pressures greater than 0.5 kbar were reproducible. As an example, figure 5 shows a typical temperature run where the sample was cooled down to 4 K and brought back to room temperature. Here, the initial pressure was 3.7 kbar at room temperature; however, it dropped to 2.1 kbar as we cross the III–IV phase boundary at 205 K. With further cooling, the pressure decreases to 1 kbar as we reach the freezing temperature of the pressure medium (about 130 K). At lower temperatures, the pressure remains practically constant. Thus, our measurements at 1 kbar, for longitudinal modes propagating perpendicular to the *c*-axis, clearly reveal two additional phase transitions below 100 K, at 64.5 ± 0.5 and 37.7 ± 0.5 K respectively. Our measurements indicate no significant thermal hysteresis at 37.7 and 64.5 K while the V–IV and IV–III phase transition are shifted at (250 K, 3.2 kbar) and (275 K, 3.3 kbar) respectively.

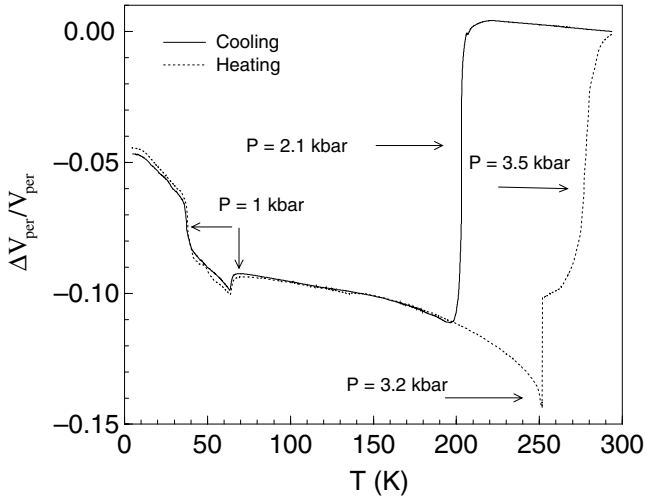

Figure 5. Temperature dependence of the sound velocity variation of longitudinal waves propagating perpendicular to the c-axis for $LiKSO_4$ obtained for an initial pressure of 3.5 kbar at room temperature.

To confirm the existence of these low-temperature phase transitions, we have also performed sound velocity measurements using longitudinal waves propagating along the c-axis. The results obtained for longitudinal modes propagating parallel and perpendicular to the c-axis are compared in figure 6. While measurements perpendicular to the c-axis show two transitions, respectively at 37.7 and 64.5 K, data along the c-direction show no sign of the transition around 37 K. Instead we observe an anomaly at 47 K with again no sign of thermal hysteresis. Only the transition at 65 K is detected for both orientations. Considering that the transition at 47 K is observed only for longitudinal waves propagating along the c-axis, it is reasonable to think that this transition involves a structural rearrangement limited to the c-axis. Similarly, the transition at 37 K probably involves a structural rearrangement limited to the a–b plane. The results in figure 6 also indicate that the variations in the velocity, observed at 37 and 47 K, decrease with increasing pressure. The critical temperatures and pressures obtained here have been included in the pressure–temperature phase diagram of $LiKSO_4$ presented in figure 4. While our phase diagram agrees with that previously obtained for temperatures above 100 K [25], our low-temperature measurements indicate that the phase transitions at 37 and 47 K vanish at pressures greater than 3.0 kbar while only the transition at 65 K remains. Our low-temperature results can only be compared to the Brillouin scattering measurements realized by Bromberek *et al* [15] down to 4 K. In their investigation at ambient pressure, the authors show that results obtained below 80 K depend on the thermal history of the sample. Nevertheless, for longitudinal acoustic modes propagating along the c-axis, they observed an increase in the velocity at $\sim$52 K that could correspond to what we observe at 47 K for a pressure of 0.4 kbar (see figure 6). The fact that they did not clearly detect the anomaly at 65 K is not surprising given that their experimental resolution, typically 1%, is about the same order of magnitude as the velocity variation measured at that temperature. Thus, their measurements are qualitatively consistent with our results. However, it is unclear why their measurements along the [100] direction do not reveal any anomalies at 38 K considering that we observe a variation of 3% in the velocity. In spite of that, IR [9], dielectric [30], EPR [31] and heat capacity [8, 32] measurements clearly support the existence of the phase transitions

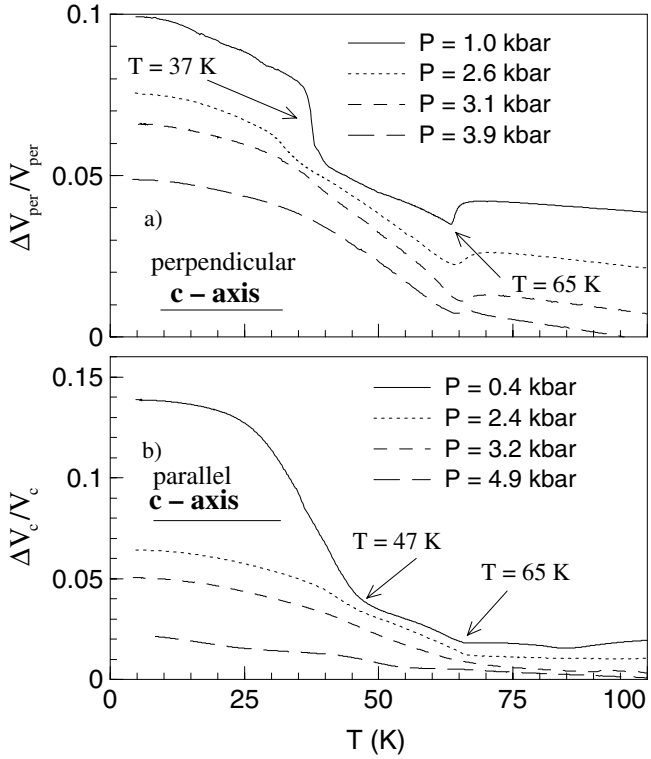

Figure 6. Temperature dependence of the relative change in sound velocity in $LiKSO_4$ at low temperatures, measured at different pressures for longitudinal modes propagating (a) perpendicular to the *c*-axis and (b) parallel to the *c*-axis. Pressures indicated here correspond to the quasi-hydrostatic pressure over that temperature range.

at 37 and 65 K. Regarding the anomaly at 47 K, only Bromberek *et al* [15] and Cach *et al* [30] mention the presence of a phase transition around that temperature. However, a close inspection of the IR results obtained by Zhang *et al* [9] clearly show the splitting of some of the S–O stretching bands that occurs between 40 and 50 K (see figures 6(a) and 7(a)). Considering that we are able to follow the evolution of all these anomalies with pressure, we believe that our results below 80 K clearly indicate the presence of three phase transitions at 65, 47 and 37 K respectively.

4. Theoretical model

So far, a few Landau models have been proposed in order to explain the elastic and dielectric properties of $LiKSO_4$ [12, 13, 25]. It turns out that none of the models that focus on the IV–V phase transition are appropriate, principally because they assumed the wrong space groups or they did not identify the proper order parameter. For example, Fujimoto *et al* [25] derived their model based on the assumption that the IV–V phase transition corresponds to a hexagonal $P6_3mc$–orthorhombic $Cmc2_1$ ferroelastic phase transition. Consequently, the free energy is expanded in terms of an order parameter which is the spontaneous strain. However, x-ray [23] and thermal expansion [25] measurements now indicate that the temperature dependence of the spontaneous strain is not that of an order parameter. Consequently, the IV–V phase transition

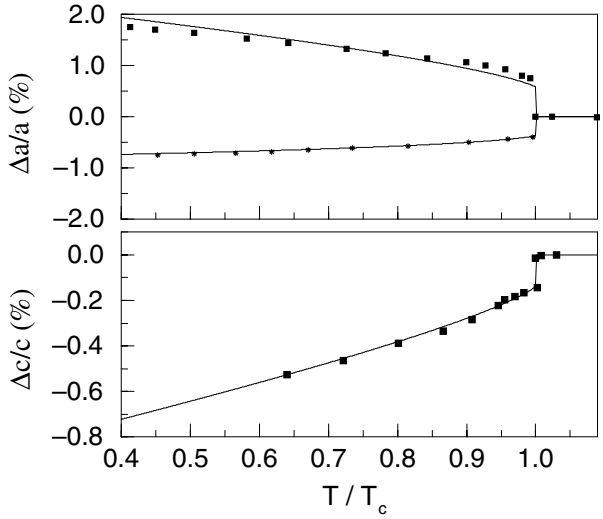

Figure 7. Temperature dependence of the strains for $LiKSO_4$. The experimental points presented in this figure are obtained from Désert *et al* [23]. The continuous curves represent fits obtained using equations (3)–(5).

cannot correspond to a proper ferroelastic transition. Mróz *et al* [13] considered a more elaborate model, but again their main assumption was that the space group sequence, going from phase III to phase V, corresponds to hexagonal $P6_3$–hexagonal $P6_3mc$–orthorhombic $Cmc2_1$. It is now well accepted that this assignment is inexact and should be replaced by hexagonal $P6_3$–trigonal $P31c$–monoclinic Cc. Therefore, here we base our analysis upon the latter phase sequence. Also, the highest symmetry structure known for $LiKSO_4$ appears above 943 K and belongs to the hexagonal space group $P6_3/mmc$ [1, 2]. The phase that exists between 708 and 943 K is known to be incommensurate and its structure still remains vague. For the purpose of this paper, in which we discuss low-temperature structures only, it is plausible to assume that the crystal does not 'remember' the highest symmetry structure for any temperature lower than 708 K. On the one hand, the $P6_3$–$P31c$ phase transition cannot be described straightforwardly in the Landau formalism, since there is no group–subgroup relationship between these space groups (the breaking of the six-fold axis symmetry at 205 K is accompanied by the appearance of mirror planes along the remaining three-fold axis). On the other hand, the Cc space group is a subgroup of $P31c$. Consequently, we assume here that it is appropriate to consider the $P6_3$(III)–$P31c$(IV)–Cc(V) transition sequence as transitions among subgroups of a hypothetical supergroup. In this case, the minimal space group which follows this criterion is $P6_3mc$ (C_{6v}^4). Thus, in table 2 we list the relevant order parameters which span the irreducible representations of the point group C_{6v} (note that at least the phases III, IV and V do not break the translational symmetry of the primitive hexagonal lattice). The order parameters which describe phase III and IV transform according to the irreducible representations $A_2(\phi)$ and $B_1(\zeta)$ of the point group C_{6v} respectively. However, the physical meaning of ϕ and ζ cannot be determined unambiguously because the assumed high-symmetry structure $P6_3mc$ is not observed. Nevertheless, considering the transformation properties of these order parameters, we can stress they do not correspond to any spontaneous strain. As a possible realization, ϕ and ζ may denote frozen amplitudes of some long-wavelength phonons [33]. For the monoclinic structure Cc, which occurs below 190 K (phase V), it

Table 2. All possible phases, described by order parameters, spanning irreducible representations A_2, B_1 and E_1 of the point group C_{6v}.

A_2, ϕ	B_1, ζ	E_1, P_x	P_y	Space group
0	0	0	0	$P6_3mc$
$\neq 0$	0	0	0	$P6_3$
0	$\neq 0$	0	0	$P31c$
0	$\neq 0$	$\neq 0$	0	Cc
$\neq 0$	$\neq 0$	0	0	$P3$
$\neq 0$	$\neq 0$	$\neq 0$	$\neq 0$	$P1$

is possible for the spontaneous polarization to be aligned along a direction that does not correspond to any particular crystallographic axis. Therefore, the spontaneous polarization in the ab plane (P_x, P_y) can be chosen as the order parameter for this transition. In the Landau free energy, we also take into account components of the strain tensor for which linear combinations correspond to the irreducible representations of C_{6v} as follows: E_2, ($e_1 - e_2$, $2e_6$), E_1, (e_4, e_5), while $e_1 + e_2$, e_3 are invariant as well as the z-component of the polarization P_z. Therefore, the model of the Landau free energy given by

$$
\begin{aligned}
F = {} & g_{\zeta 1}\zeta^2 + g_{\zeta 2}\zeta^4 + g_{\phi 1}\phi^2 + g_{\phi 2}\phi^4 + g_{\zeta\phi}\zeta^2\phi^2 \\
& + a_1(P_x^2 + P_y^2) + a_2(P_x^2 + P_y^2)^2 + b(P_x^3 - 3P_xP_y^2)\zeta + d_1P_z + \frac{P_z^2}{2\chi_z^o} \\
& + f_1(P_x^2 + P_y^2)^2P_z + f_2(P_x^3 - 3P_xP_y^2)\zeta P_z \\
& + \tfrac{1}{2}C_{33}^o e_3^2 + \tfrac{1}{4}(C_{11}^o + C_{12}^o)(e_1 + e_2)^2 + \tfrac{1}{4}(C_{11}^o - C_{12}^o)[(e_1 - e_2)^2 + 4e_6^2] \\
& + C_{13}^o(e_1 + e_2)e_3 + c_{14}[(e_1 - e_2)e_4 - 2e_5e_6]\zeta + \tfrac{1}{2}C_{44}^o(e_4^2 + e_5^2) \\
& + \mu_1(P_xe_4 + P_ye_5) + \mu_2\zeta[P_x(e_1 - e_2) - 2P_ye_6] \\
& + \nu_1(P_x^2 + P_y^2)(e_1 + e_2) + \nu_2(P_x^2 + P_y^2)e_3 \\
& + \nu_3[(P_x^2 - P_y^2)(e_1 - e_2) + 4P_xP_ye_6] + \nu_4\zeta[(P_x^2 - P_y^2)e_4 - 2P_xP_ye_5], \qquad (1)
\end{aligned}
$$

is a good starting point in order to describe the low-temperature phase transitions observed for $LiKSO_4$. Here, terms in the first line account for phases III and IV and the coupling term $g_{\zeta\phi}\zeta^2\phi^2$ is necessary in order to describe the direct phase transition between them. Terms associated with the polarization energy as well as the coupling terms between the polarization and ζ are all given in the second and third lines. The remaining lines contain elastic energy terms as well as various coupling terms which involve the different strain components. In principle, this model can be used to account for the phase diagram (assuming some temperature and pressure dependence of the coefficients), which contains phases listed in table 2. Anomalies of such quantities as elastic modulus, dielectric and piezoelectric constants can be calculated.

The main purpose of this theoretical section is to show that this Landau free energy describes remarkably well the elastic and dielectric properties of $LiKSO_4$ at the IV–V phase boundary. We leave the complete consideration of the model (1) for further theoretical studies. Here, we consider a simplified model which concentrates on the $P31c$(IV)–Cc(V) phase transition. As indicated in table 2, we simultaneously have that $\phi = P_y = 0$, and $\zeta \neq 0$ in phases $P31c$(IV) and Cc(V). Moreover, we can assume that around the IV to V transition point ζ has reached its saturated value and remains constant. Consequently, the only parameter which differentiates both phases is the x-axis component of the polarization which must correspond to the order parameter Q ($P_x \equiv Q$). After neglecting any coupling terms which involve shear

strain components, the expression for the free energy reduces to

$$F_{\mathrm{IV-V}}(Q, e_i, P_z) = a_1 Q^2 + a_2 Q^4 + b' Q^3 + d_1 P_z + \frac{P_z^2}{2\chi_z^o} + f_1 Q^4 P_z + f_2' Q^3 P_z + \tfrac{1}{2} C_{11}^o (e_1^2 + e_2^2) + \tfrac{1}{2} C_{33}^o e_3^2 + C_{12}^o e_1 e_2 + C_{13}^o (e_1 + e_2) e_3 + \mu_2' Q (e_1 - e_2) + \nu_1 Q^2 (e_1 + e_2) + \nu_2 Q^2 e_3 + \nu_3 Q^2 (e_1 - e_2), \quad (2)$$

where $b' = b\zeta$, $f_2' = f_2\zeta$ and $\mu_2' = \mu_2\zeta$. From the minimization of the free energy with respect to e_i and P_z, we easily obtain the expressions for the spontaneous strains $e_i(Q)$ and the z-component of the polarization $P_z(Q)$ which correspond to

$$e_1(Q) = -\frac{\mu_2' Q + (\nu_1 + \nu_3) Q^2}{C_{11}^o} \quad (3)$$

$$e_2(Q) = \frac{\mu_2' Q + (-\nu_1 + \nu_3) Q^2}{C_{11}^o} \quad (4)$$

$$e_3(Q) = -\frac{\nu_2 Q^2}{C_{33}^o} \quad (5)$$

$$P_z(Q) = -\chi_z^o (d_1 + f_1 Q^2 + f_2' Q^3). \quad (6)$$

We immediately see that the solution for $P_z(Q)$ predicts a non-vanishing polarization, even above the phase transition, $P_z(IV) = -d_1 \chi_z^o$. This prediction is in fact consistent with experimental results on $P_z(T)$ [25]. Now, using the expression for the polarization, it is straightforward to derive an effective Landau free energy $F_{\mathrm{eff}}(Q, e_i)$ from which the elastic constant can be obtained. The effective free energy can be written as

$$F_{\mathrm{eff}}(Q, e_i) = \tfrac{1}{2}\alpha(T) Q^2 - \tfrac{1}{3}\beta Q^3 + \tfrac{1}{4}\gamma Q^4 + \tfrac{1}{2} C_{11}^o (e_1^2 + e_2^2) + \tfrac{1}{2} C_{33}^o e_3^2 + \mu_2' Q (e_1 - e_2) + \nu_1 Q^2 (e_1 + e_2) + \nu_2 Q^2 e_3 + \nu_3 Q^2 (e_1 - e_2), \quad (7)$$

where $\alpha(T) = 2(a_1(T) - d_1 f_1 \chi_z^o)$, $\beta = -3(b' - d_1 f_2' \chi_z^o)$ and $\gamma = 4a_2 - 2f_1^2 \chi_z^o$ are the usual Landau expansion coefficients for a first-order transition and C_{ij}^o are the elastic constants associated with $P6_3mc$. Here, higher-order terms proportional to Q^5 and Q^6 have been neglected for convenience. This effective free energy can readily be used to calculate the elastic constants using [34]

$$C_{mn} = \frac{\partial^2 F(Q, e_i)}{\partial e_m \partial e_n} - \frac{\partial^2 F(Q, e_i)}{\partial Q \partial e_m} \left(\frac{\partial^2 F(Q, e_i)}{\partial Q^2} \right)^{-1} \frac{\partial^2 F(Q, e_i)}{\partial e_n \partial Q}. \quad (8)$$

For simplicity, we limit our analysis to measurements along the c-axis. Along that particular direction, the velocity of longitudinal waves, in both phases, is simply given by

$$V_c = \sqrt{\frac{C_{33}}{\rho}}.$$

Using the expression of effective free energy $F_{\mathrm{eff}}(Q, e_i)$ and equation (8), we obtain for the elastic constant C_{33}

$$C_{33}(Q) = C_{33}^o - \frac{4\nu_2^2 Q^2}{\frac{2\mu_2'^2}{C_{11}^o} + (\frac{2\mu_2'\nu_3}{C_{11}^o} - \beta) Q + 2\gamma Q^2}. \quad (9)$$

Instead of arbitrarily adjusting all these parameters, we have chosen to use the existing experimental data to find a self-consistent solution. In fact, most coefficients entering in this model can be easily obtained by first fitting the temperature dependence of the strain

Table 3. Values of the parameters used to fit the strains, C_{33} and ϵ_3.

$\nu_1 = -0.81$	$\nu_2 = 10.2$	$\nu_3 = 0.65$	$\mu'_2 = 0.66$	$\chi_3^o = 6.0$	$b' = -0.076$
$a_2 = 0.2$	$d_1 = -0.0067$	$f_1 = 0.05$	$f_2 = 0.03$	$C_{33} = 1000$	$C_{11} = 60$

components. The results of these fits are reproduced in figure 7 along with experimental data obtained by Désert *et al* [23]. The last parameter can then be used to reproduce the velocity variation observed at T_c. The results of this procedure are presented in figure 8 where we compare the velocity variation obtained along the c-axis (squares) with the prediction based on equation (9) (continuous curve). We also present (see inset), the resulting temperature dependence obtained for the elastic constant C_{11}. Considering that, the velocity of longitudinal waves propagating perpendicular to the c-axis depends on C_{11}, along with other elastic constants (C_{16}, C_{66}, C_{22}, C_{26}), it is not surprising that the temperature dependence of C_{11} does not exactly reproduce the experimental results presented in figure 3(a). However, it does show a softening as temperature is increased up to the critical temperature T_c followed by a sudden increase. It also shows a quasi-linear dependence above T_c which is consistent with the temperature dependence of the velocity for longitudinal waves propagating perpendicular to the c-axis. Finally, considering that our model also takes into account the coupling with the polarization, we did not limit our analysis to the elastic properties. The same model can be used to calculate the relative permittivity along the c-axis, ϵ_3. Again, one first needs to derive an effective free energy $F(Q, P)$ using equations (2) and (3)–(5). From that effective free energy, the dielectric susceptibility, χ_3, can be derived using

$$\frac{1}{\chi_3} = \frac{1}{\epsilon_3 - 1} = \frac{\partial^2 F(Q, P_z)}{\partial P_z^2} - \left(\frac{\partial^2 F(Q, P_z)}{\partial Q \partial P_z}\right)^2 \Bigg/ \left(\frac{\partial^2 F(Q, P_z)}{\partial Q^2}\right) \tag{10}$$

from which we obtain

$$\frac{1}{\chi_3(Q)} = \frac{1}{\chi_3^o} - \frac{Q(2f_1 + 3Qf_2')^2}{\sigma_0 + \sigma_1 Q} \tag{11}$$

where

$$\sigma_0 = -\beta + \frac{6\mu'_2 \nu_3}{C_{11}^o}$$

$$\sigma_1 = 2\gamma + 4f_1^2 \chi_3^o - \frac{4\nu_2^2}{C_{33}^o} - \frac{8(\nu_1^2 + \nu_3^2)}{C_{11}^o}.$$

Thus, using the same set of parameters, we present in figure 9 a comparison between the prediction derived from equation (10) and the experimental data obtained by Cach *et al* [30]. Again, the agreement between the prediction based on our model and the experimental result is remarkable. The values of the parameters used in all the fits presented here can be found in table 3.

5. Conclusions

In summary, our high-resolution sound velocity measurements under pressure confirm the existence of five phase transitions (37, 47, 62, 187 and 195 K, on heating) between 4 K and room temperature. In comparison with the sequence of phases presented in figure 2, we did not observe any anomalies at 135 or 165 K, either for elastic waves propagating along or perpendicular to the c-axis (see figures 2, 3 and 5). So far, experimental evidence that supports these two phase transitions is scarce and the physical anomalies associated with it are

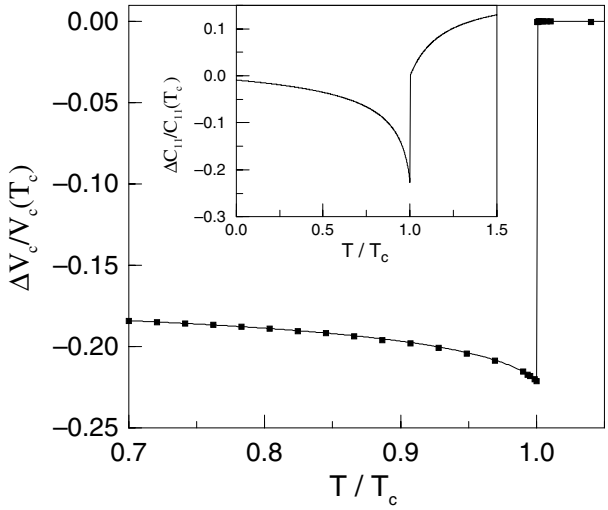

Figure 8. Temperature dependence of the velocity variation measured along the *c*-axis using longitudinal waves propagating in $LiKSO_4$ (the data points presented here are taken from figure 2). The continuous curve represents the fit obtained using equation (9). The inset presents the temperature dependence of C_{11} as predicted by our Landau model, equation (7).

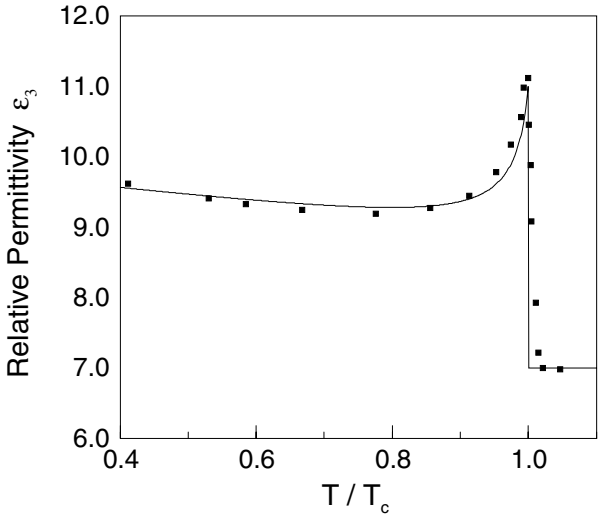

Figure 9. Temperature dependence of the relative permittivity of $LiKSO_4$ along the *c*-axis. The data points presented here are obtained from Cach *et al* [30]. The continuous curve is obtained using equation (11).

faint. Moreover, the variations take place through an extended temperature range instead of a sudden change at the critical temperature. Considering that sound velocity measurements are especially sensitive to the static properties of the crystal, our results suggest that the anomalies at 135 and 165 K are possibly related to a variation in the dynamic properties rather than a structural change. We have also derived the pressure–temperature phase diagram of $LiKSO_4$ for temperatures between 4 and 300 K. Our results indicate that the phase transitions at 37 and 47 K are both easily suppressed under pressure. More importantly, our investigation clearly

demonstrates that it is possible to obtain reproducible results at low temperatures, without any special heat treatment, as long as a minimum pressure of 0.5 kbar is maintained on the sample. This suggests that it might be possible to elucidate the structure of the low-temperature phases if the measurements are made under hydrostatic pressure.

In this paper we also present a Landau model which is derived using the group theory. We particularly focus on the $P31c$(IV)–Cc(V) phase transition for which reliable experimental data are available. Our model indicates that the actual order parameter associated with this transition corresponds to the spontaneous polarization in the *ab* plane. This is supported by the very good agreement that we obtain between the theoretical predictions and the observed temperature dependence of the strains (e_1, e_2, e_3), the polarizations (P_3, not shown here), the dielectric susceptibility (χ_3) and the sound velocity variation along the c-axis ($\Delta V_c/V_c$ for longitudinal waves). Unfortunately, regarding the phase transitions observed below 80 K, because of the ambiguity that still exists with respect to the space groups and the lack of reliable data in this temperature range, it is difficult to derive any coherent model. Additional experimental work is required in this temperature range before the order parameters can be identified.

Acknowledgments

This work was supported by grants from the Natural Science and Engineering Research Council of Canada (NSERC) and Canada Foundation for Innovation (CFI). It has been also partially supported by the grant no 5 P03B 027 21 from the Polish State Committee for Scientific Research.

References

[1] Li Y Y 1984 *Solid State Commun.* **51** 355
[2] Chung S J and Hahn T 1972 *Acta Crystallogr.* A **28** 557
[3] Bradley A 1925 *Phil. Mag.* **49** 1225
[4] Schulz H, Zucker U and Frech R 1985 *Acta Crystallogr.* B **41** 21
[5] Bansal M L and Roy A P 1984 *Phys. Rev.* B **30** 7307
[6] Rajagopal H, Java V, Sequeira A and Chidambaram R 1991 *Physica* B **174** 95
[7] Bhakay-Tamhane S, Sequeira A and Chidambaram R 1991 *Solid State Commun.* **53** 197
[8] Abello L, Chhor K and Pommier C 1985 *J. Chem. Thermodyn.* **17** 1023
[9] Zhang M, Salje E and Putnis A 1998 *J. Phys.: Condens. Matter* **10** 11811
[10] Perpétuo G J, Dantas M S S, Gazzinelli R and Pimenta M A 1992 *Phys. Rev.* B **45** 5163
[11] Pimenta M A, Lustin Y and Hauret G 1987 *Solid State Commun.* **62** 275
[12] Tu A, Liu J-Q, Gu B-Y, Mo Y-J, Yang H-G and Wang Y-Y 1987 *Solid State Commun.* **61** 1
[13] Mróz B, Tuszyński J A, Kiefte H and Clouter M J 1989 *J. Phys.: Condens. Matter* **1** 5965
[14] Drozdowski M and Holuj F 1988 *Ferroelectrics* **77** 47
[15] Bromberek M, Clouter M J and Mróz B 2002 *J. Phys.: Condens. Matter* **14** 5135
[16] Ganot F, Kihal B, Dugautier C, Farhi R and Moch P 1987 *J. Phys. C: Solid State Phys.* **20** 4491
[17] Mróz B, Krajewski T, Breczewski T, Chomka W and Sematowicz D 1982 *Ferroelectrics* **42** 71
[18] Borisov B F, Charnaya E V and Radzhabov A K 1996 *Ferroelectrics* **185** 161
[19] Willis F, Leisure R and Kanashiro T 1996 *Phys. Rev.* B **54** 9077
[20] Kabelka H and Kuchler G 1988 *Ferroelectrics* **88** 93
[21] Borisov B F, Charnaya E V and Vinogradova M Y 1997 *Phys. Status Solidi* b **199** 51
[22] Tomaszewski P E and Lukaszewicz K 1983 *Phase Transit.* **4** 37
[23] Désert A, Gibaud A, Righi A, Leitão U A and Moreira R L 1995 *J. Phys.: Condens. Matter* **7** 8445
[24] Godfrey L and Philip J 1996 *Solid State Commun.* **97** 635
[25] Fujimoto S, Yasuda N and Hibino H 1985 *J. Phys. D: Appl. Phys.* **18** 1871
[26] Oliveira A J, Germano F A, Filho J M and Moreira J E 1988 *Phys. Rev.* B **38** 12633
[27] Fujimoto S, Yasuda N and Hibino H 1984 *Phys. Lett.* A **104** 42

[28] Melo F E A, Lemos V, Cerdeira F and Filho J M 1987 *Phys. Rev.* B **35** 3633
[29] Sankaran H, Sharma S M and Sikka S K 1988 *Solid State Commun.* **66** 7
[30] Cach R, Tomaszewski P and Bornarel J 1985 *J. Phys. C: Solid State Phys.* **18** 915
[31] Bill H, Sekhar Y R and Lovy D 1988 *J. Phys. C: Solid State Phys.* **21** 2795
[32] Diosa J E, Gonalez-Montero G and Vargas R A 2000 *Phys. Status Solidi* b **220** 647
[33] Sergienko I A and Curnoe S H 2003 *J. Phys. Soc. Japan* at press
[34] Rehwald W 1973 *Adv. Phys.* **22** 721